Available online at www.sciencedirect.com
SCIENCE DIRECT
NeuroToxicology 27 (2006) 82–92
NeuroToxicology

Acute neurotoxic effects of the fungal metabolite ochratoxin-A

V. Sava [a,c], O. Reunova [a,c], A. Velasquez [a,c], R. Harbison [b], J. Sánchez-Ramos [a,c,*]

[a] University of South Florida, Department of Neurology (MDC 55), 12901 Bruce B. Downs Blvd., Tampa, FL 33612, USA
[b] College of Public Health, University of South Florida, Tampa, FL, USA
[c] Research Service, James Haley VA, Tampa, FL, USA

Received 31 January 2005; accepted 12 July 2005
Available online 2 September 2005

Abstract

Ochratoxin-A (OTA) is a fungal metabolite with potential toxic effects on the central nervous system that have not yet been fully characterized. OTA has complex mechanisms of action that include evocation of oxidative stress, bioenergetic compromise, inhibition of protein synthesis, production of DNA single-strand breaks and formation of OTA–DNA adducts. The time course of acute effects of OTA were investigated in the context of DNA damage, DNA repair and global oxidative stress across six brain regions. Oxidative DNA damage, as measured with the ''comet assay'', was significantly increased in the six brain regions at all time points up to 72 h, with peak effects noted at 24 h in midbrain (MB), CP (caudate/putamen) and HP (hippocampus). Oxidative DNA repair activity (oxyguanosine glycosylase or OGG1) was inhibited in all regions at 6 h, but recovered to control levels in cerebellum (CB) by 72 h, and showed a trend to recovery in other regions of brain. Other indices of oxidative stress were also elevated. Lipid peroxidation and superoxide dismutase (SOD) increased over time throughout the brain. In light of the known vulnerability of the nigro-striatal dopaminergic neurons to oxidative stress, levels of striatal dopamine (DA) and its metabolites were also measured. Administration of OTA (0–6 mg/kg i.p.) to mice resulted in a dose-dependent decrease in striatal DA content and turnover with an ED50 of 3.2 mg/kg. A single dose of 3.5 mg/kg decreased the intensity of tyrosine hydroxylase immunoreactivity (TH+) in fibers of striatum, TH+ cells in substantia nigra (SN) and TH+ cells of the locus ceruleus. TUNEL staining did not reveal apoptotic profiles in MB, CP or in other brain regions and did not alter DARPP32 immunoreactivity in striatum. In conclusion, OTA caused acute depletion of striatal DA on a background of globally increased oxidative stress and transient inhibition of oxidative DNA repair.

Keywords: Ochratoxin-A; Oxyguanosine glycosylase; Superoxide dismutase; Dopamine; Tyrosine hydroxylase; Apoptosis; Substantia nigra; Striatum

1. Introduction

Ochratoxin-A (OTA) is a metabolite produced by *Aspergillus ochraceus* and *Penicillium verrucosum* that accumulates in the food chain because of its long half-life (Galtier, 1991; Kuiper-Goodman and Scott, 1989). In view of its ubiquity, the possible contribution of OTA to the development of human and animal diseases has been investigated (see review Marquardt and Frohlich, 1992). OTA has been shown to induce a tubulointerstitial nephropathy in animals (Krogh et al., 1974) and enzymuria (Kane et al., 1986a,b) similar to Balkan endemic nephropathy found in humans (Krogh, 1992; Krogh et al., 1974; Petkova-Bocharova et al., 1988). In addition to nephrotoxicity, OTA disrupts blood coagulation (Galtier et al., 1979; Gupta et al., 1979) and glucose metabolism (Pitout, 1968). It is immunosuppressive (Creppy et al., 1983b; Haubeck et al., 1981; Lea et al., 1989; Stormer and Lea, 1995), teratogenic (Arora et al., 1983; Fukui et al., 1992; Szczech and Hood, 1981) and genotoxic (Creppy et al., 1985; Pfohl-Leszkowicz et al., 1991).

Investigation of the effects of acute and chronic exposure to OTA on the nervous system has been scarce, even though development of nervous tissue appears to be very susceptible to the deleterious effects of OTA (Hayes et al., 1974; Wangikar et al., 2004). OTA has been reported to induce teratogenic effects in neonates (rats and mice) exposed in utero, characterized by microcephaly and modification of the brain levels of free amino acids (Belmadani et al., 1998). OTA was also reported to be neurotoxic to adult male rats fed OTA in the diet. Neurotoxicity, indicated by concentration of lactic dehydrogenase released from the dissected brain tissue, was more pronounced in the ventral mesencephalon, hippocampus, and striatum than in the cerebellum (Belmadani et al., 1998).

* Corresponding author. Tel.: +1 813 974 6022; fax: +1 813 974 7200.
E-mail address: jsramos@hsc.usf.edu (J. Sánchez-Ramos).

0161-813X/$ – see front matter © 2005 Elsevier Inc. All rights reserved.
doi:10.1016/j.neuro.2005.07.004

The bio-concentration of OTA in these brain regions did not correlate with toxicity (Belmadani et al., 1998).

The mechanism responsible for toxicity to neural tissues is not clear, but studies in peripheral organs and tissues reveal a spectrum of actions. The mechanisms of toxicity implicated include inhibition of protein synthesis, mitochondrial impairment, oxidative stress and DNA damage (Creppy et al., 1985, 1990; Dirheimer and Creppy, 1991; Gautier et al., 2001).

OTA-induced damage to DNA, evidenced by formation of single-strand breaks, has been reported to occur both in vitro and in vivo (Creppy et al., 1985). The DNA damage was shown to be reversible with time suggesting that variation in capacity to repair DNA may account in part for differences in vulnerability to OTA between tissues. OTA was also reported to induce single-strand breaks in a concentration-dependent manner in canine kidney cells and this effect could be potentiated by inhibition of DNA repair (Lebrun and Follmann, 2002). Other studies have demonstrated OTA–DNA adducts in mouse and monkey kidney after OTA treatment (Grosse et al., 1995). In kidney, liver and spleen, several modified nucleotides were clearly detected in DNA, 24 h after administration of OTA, but their levels varied significantly in a tissue and time-dependent manner over a 16-day period. The OTA–DNA adducts were not quantitatively and qualitatively the same in the three organs examined due to differences of metabolism in these organs and differences in the efficiency of DNA repair processes (Pfohl-Leszkowicz et al., 1993).

OTA treatment can increase oxidative stress in peripheral organs. Administration of OTA (1 mg/kg) to rats resulted in a 22% decrease in alpha-tocopherol plasma levels and a five-fold increase in the expression of the oxidative stress responsive protein heme oxygenase-1, specifically in the kidney (Gautier et al., 2001). More direct evidence of oxidative stress was derived from studies, which utilized electron paramagnetic resonance spectroscopy to measure the generation of hydroxyl radicals, in rat hepatocyte mitochondria and microsomes incubated with OTA and metabolites (Hoehler et al., 1997).

OTA toxicity is associated with inhibition of both protein and RNA synthesis (Dirheimer and Creppy, 1991). OTA is known to interfere with the charging of transfer ribonucleic acids (tRNA) with amino acids (Dirheimer and Creppy, 1991). In particular, OTA has been shown to inhibit bacterial, yeast and liver phenylalanyl-tRNA synthetases (Dirheimer and Creppy, 1991). The inhibition is competitive to phenylalanine and is reversed by an excess of this amino acid. OTA has also been shown to inhibit enzymes that use phenylalanine as a substrate such as phenylalanine hydroxylase (Dirheimer and Creppy, 1991).

Mitochondrial dysfunction has been shown to be involved in the development of OTA-induced toxicity in proximal renal tubule cells (Aleo et al., 1991). Respiration was reduced in the absence and presence of a phosphate acceptor using site I (glutamate/malate) and site II (succinate) respiratory substrates 15 and 30 min after exposure to 10^{-3} M OTA, implicating an action of OTA at both electron transport sites (Aleo et al., 1991). However, in isolated rat liver mitochondria, inhibition kinetic studies revealed that OTA is an uncompetitive inhibitor of both succinate-cytochrome *c* reductase and succinate dehydrogenase while sparing cytochrome oxidase and NADH dehydrogenase activity (Complex I) at concentrations less than 10^{-5} M (Wei et al., 1985).

The objective of the present study was to evaluate the extent of OTA neurotoxicity across mouse brain regions in the context of oxidative stress, oxidative DNA damage and DNA repair. Deficits in DNA repair have long been implicated in a number of neurodegenerative diseases, including Alzheimer's disease and Parkinson's disease. It was our goal to determine whether regional differences in DNA repair capacity predicts vulnerability to the toxin. We hypothesized that OTA-induced oxidative DNA damage would not be homogeneous across all brain regions but would reflect the capacity of distinct regions of brain to respond with antioxidative repair processes. Given the body of evidence that nigro-striatal DA neurons are especially vulnerable to oxidative stress, we also hypothesized that DA levels in striatum would be affected by OTA. Hence, we measured the effects of OTA on striatal dopamine (DA) levels and parameters of oxidative stress in six brain regions cerebellum (CB), cortex (CX), hippocampus (HP), midbrain (MB), caudate/putamen (CP) and pons/medulla (PM). Parameters of oxidative stress measured included lipid peroxidation (thiobarbituric acid-reactive substances or TBARS), SOD activity, oxidative DNA damage and repair. The enzymatic activity of DNA glycosylase served as the index of DNA repair.

2. Materials and methods

2.1. Materials

Ochratoxin-A, SOD and dihydrobenzylamine were purchased from Sigma (St. Louis, MO). Protease inhibitors and DNA glycosylase were from Boehringer Mannheim (Indianapolis, IN, USA). ^{32}P-ATP was from NEN Life Science Products (Wilmington, DE). Rabbit anti-tyrosine hydroxylase was purchased from Pel-Freez Biologicals (Arkansas, AR). Rabbit primary antibodies to DARPP32 (dopamine and cyclic AMP regulated phosphoprotein) were purchased from Chemicon, CA. ApopTag in situ Apoptosis Detection Kit and goat anti-rabbit secondary antibody were from Chemicon, CA. All other reagents were from Sigma Chemical Co.

2.2. Animals and treatment

The animal protocol used in this study was approved by the University of South Florida IUCAC committee. The protocol was also reviewed and approved by the Division of Comparative Medicine of the University, which is fully accredited by AAALAC International and managed in accordance with the Animal Welfare Regulations, the PHS Policy, the FDA Good Laboratory Practices, and the IACUC's Policies.

Male Swiss ICR mice (22 ± 2 g) were obtained from the Jackson Laboratories (Bar Harbor, ME). They were housed five per cage at the temperature of 21 ± 2 °C with 12 light/dark

cycle and free access to food and water. Mice were divided into experimental (total $n = 70$) and control (total $n = 20$) groups. Animals were injected with either OTA dissolved in 0.1 M $NaHCO_3$ mg/kg i.p. or vehicle (0.1 M $NaHCO_3$). After injection with OTA or vehicle, mice were observed for changes in spontaneous behavior three times each day until euthanasia. The response to handling was also noted. In particular, evidence for toxic effects such as clasping of limbs in response to being held by the tail was to be recorded. Groups of mice were euthanatized with CO_2 at 6, 24, and 72 h after injection with OTA or vehicle. The brains were removed and immediately dissected on ice.

2.3. Isolation of brain regions

Brains were separated into six regions under a dissecting stereo-microscope in the following order. The cerebellar peduncles were cut first, and brain stem was removed from the diencephalon. The ventral and dorsal parts of midbrain (MB) were dissected at the level of the caudal end of the cerebral peduncles at the junction with the pons. The pons and medulla (PM) were separated together by cutting the ponto-medullary junction. The cerebral hemispheres were opened with a sagittal cut along the longitudinal tissue and hippocampus (HP) was isolated, followed by caudate and putamen (CP). Finally, cerebellum (CB) and cerebral cortex (CX) were harvested and all the samples were kept frozen at −70 °C until assayed (see Fig. 1).

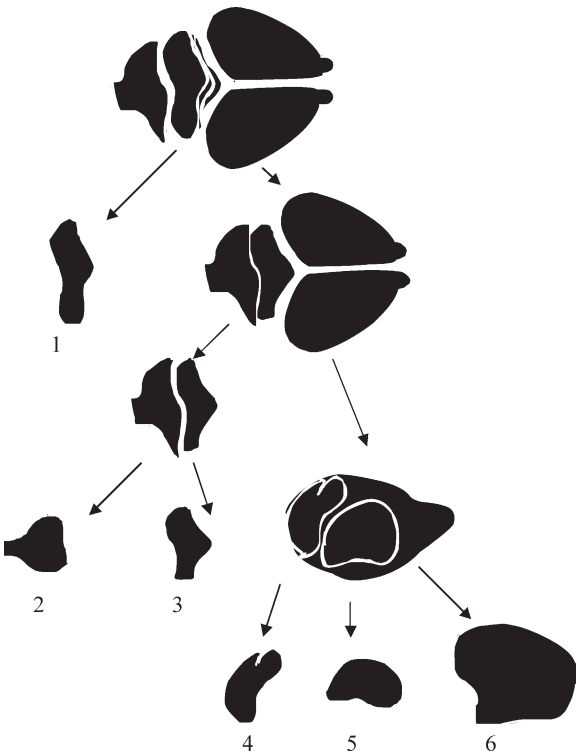

Fig. 1. Each mouse brain was dissected on ice under a stereo-microscope into six regions: (1) cerebellum (CB); (2) pons/medulla (PM); (3) midbrain (MB); (4) hippocampus (HP); (5) caudate/putamen (CP); (6) cerebral cortex (CX).

2.4. Evaluation of OTA neurotoxicity

Mice of either sex were distributed into six groups containing eight animals with an equal number of both sexes in each group. The first group of untreated animals was considered as a control, and the other five groups were treated with OTA given intraperitoneally in doses of 0–6 mg/kg of body weight. Striatal dopamine concentration was measured with HPLC 24 h after OTA administration, and the dose that caused 50% reduction in striatal DA concentrations (ED50) was calculated using the GraphPad Software, Inc. (Sorrento, CA). The ED50 was determined for eight animals in each group.

2.5. DNA damage evaluated by the comet assay

The comet assay was based on a modification of a previously published method (Schindewolf et al., 2000). Two layers of agarose were prepared. For the first layer, 85 μL 1% (w/v) high-melting point (HMP) agarose (Sigma) prepared at 95 °C in PBS was pipetted onto fully frosted microscope slides, covered with coverslip and allowed to set at 4 °C for 10 min. Cells were dissociated with 3% trypsin and RNAse following washing in PBS, centrifuged at $700 \times g$ for 15 min and resuspended at 2×10^5 in 85 μL 1% (w/v) low-melting point (LMP) agarose (Sigma). The cell suspension was then pipetted over the set HMP agarose layer, covered with coverslip and allowed to set at 4 °C for 10 min. After the coverslips were removed, the slides were immersed in pre-chilled lysis solution [2.5 M NaCl, 100 mM sodium EDTA, 10 mM Tris, pH adjusted to 10 using NaOH pellets, 1% Triton X-100 (v/v) (added immediately before use)] for 60 min at 4 °C to remove cellular proteins. Following lysis, slides were placed in a gel electrophoresis unit and incubated in fresh alkaline electrophoresis buffer (300 mM NaOH, 1 mM EDTA, pH 13) for 40 min at room temperature, before being electrophoresed at 25 V (300 mA) for 30 min at 4 °C. All the above procedures were conducted in the dark to minimize extraneous sources of DNA damage. Following electrophoresis, the slides were immersed in neutralization buffer (0.4 M Tris–HCl, pH 7.5) and gently washed three times for 5 min at 4 °C to remove alkalis and detergents. SYBR Green (50 μL; Trevigen, Gaithersburg, MD) was added to each slide to stain the DNA, then covered with a coverslip and kept in the dark before viewing. Slides were examined at 250× magnification on a Zeiss inverted fluorescence microscope (Zeiss, Germany) at 460 nm. One hundred randomly selected nonoverlapping cells were visually assigned a score based on perceived comet tail length migration and relative proportion of DNA in the comet tail. The extent of DNA damage was calculated as follows:

$$\text{DNA damage} = \text{tail length}/\text{diameter of comet head}.$$

2.6. Assessment OGG1 activity

The procedure for extraction of DNA glycosylase was similar to that described previously (Cardozo-Pelaez et al., 2000). Punched tissues were sonicated in homogenization

buffer containing 20 mM Tris, pH 8.0, 1 mM EDTA, 1 mM dithiothrietol (DTT), 0.5 mM spermine, 0.5 mM spermidine, 50% glycerol and protease inhibitors and homogenates were rocked for 30 min after addition of 1/10 volume of 2.5 M KCl. Samples were spun at 14,000 rpm for 30 min and supernatants were collected.

The OGG1 activities in supernatants were determined using duplex oligonucleotide containing 8-oxodG as incision substrate. For preparation of the incision assay, 20 pmol of synthetic probe containing 8-oxodG (Trevigen, Gaithersburg, MD) was labeled with ^{32}P at the 5′ end using polynucleotide T4 kinase (Boehringer Mannheim, Germany). Unincorporated free ^{32}P-ATP was separated on G25 spin column (Prime; Inc., Boulder, CO). Complementary oligonucleotides were annealed in 10 mM Tris, pH 7.8, 100 mM KCl, 1 mM EDTA by heating the samples 5 min at 80 °C and gradually cooling at room temperature.

Incision reactions were carried out in a mixture (20 μL) containing 40 mM HEPES (pH 7.6), 5 mM EDTA, 1 mM DTT, 75 mM KCl, purified bovine serum albumin, 100 fmol of ^{32}P-labeled duplex oligonucleotide, and extracted guanosine glycosylase (30 μg of protein). The reaction mixture was incubated at 37 °C for 2 h and products of the reaction were analyzed on denaturing 20% polyacrylamide gel. Pure OGG1 served as positive control and untreated duplex oligonucleotide was used for negative control. The gel was visualized with a Biorad-363 Phosphoimager System. The incision activity of OGG1 was calculated as the amount of radioactivity in the band representing specific cleavage of the labeled oligonucleotide over the total radioactivity. Data were normalized to equal concentration of protein, the concentration of which was measured using the bicinchoninic acid assay (Smith et al., 1985).

2.7. SOD assay

Determination of superoxide dismutase activity in mouse brain was based on inhibition of nitrite formation in reaction of oxidation of hydroxylammonium with superoxide anion radical (Elstner and Heupel, 1976). Nitrite formation was generated in a mixture contained 25 μL xanthine (15 mM), 25 μL hydroxylammonium chloride (10 mM), 250 μL phosphate buffer (65 mM, pH 7.8), 90 μL distilled water and 100 μL xanthine oxidase (0.1 U/mL) used as a starter of the reaction. Inhibitory effect of inherent SOD was assayed at 25 °C during 20 min of incubation with 10 μL of brain tissue extracts. Determination of the resulted nitrite was performed upon the reaction (20 min at room temperature) with 0.5 mL sulfanilic acid (3.3 mg/mL) and 0.5 mL α-naphthylamine (1 mg/mL). Optical absorbance at 530 nm was measured on Ultrospec III spectrophotometer (Pharmacia, LKB). The results were expressed as units of SOD activity calculated per milligram of protein. The amount of protein in the samples was determined using the bicinchoninic acid (Smith et al., 1985).

2.8. Lipid peroxidation assay

Formation of lipid peroxide derivatives was evaluated by measuring thiobarbituric acid-reactive substances (TBARS) according to a previously reported method (Cascio et al., 2000). Briefly, the different regions of brain were individually homogenized in ice-cold 1.15% KCl (w/v); then 0.4 mL of the homogenates were mixed with 1 mL of 0.375% TBA, 15% TCA (w/v), 0.25N HCl and 6.8 mM butylated-hydroxytoluene (BHT), placed in a boiling water bath for 10 min, removed and allowed to cool on ice. Following centrifugation at 3000 rpm for 10 min, the absorbance in the supernatants was measured at 532 nm. The amount of TBARS produced was expressed as nmol TBARS/mg protein using malondialdehyde bis(dimethyl acetal) for calibration.

2.9. Measurement of dopamine and metabolites

HPLC with electrochemical detection was employed to measure levels of dopamine (DA) as previously reported in our laboratory (Cardozo-Pelaez et al., 1999). Tissue samples were sonicated in 50 volumes of 0.1 M perchloric acid containing 50 ng/mL of dihydrobenzylamine (Sigma Chemical, MA) as internal standard. After centrifugation (15,000 × *g*, 10 min, 4 °C), 20 μL of supernatant was injected onto a C18-reversed phase RP-80 catecholamine column (ESA, Bedford, MA). The mobile phase consisted of 90% of a solution of 50 mM sodium phosphate, 0.2 mM EDTA, and 1.2 mM heptanesulfonic acid (pH 4) and 10% methanol. Flow rate was 1.0 mL/min. Peaks were detected by a Coulchem 5100A detector (ESA). Data were collected and processed with TotalChrom software (Perkin Elmer Instruments).

2.10. Tissue preparation

Mice were euthanatized after 72 h of a single injection with OTA. They were then perfused via the heart and ascending aorta with 25 mL ice-cold phosphate buffered saline (0.1 M PBS), followed by 50 mL freshly prepared 4% paraformaldehyde in PBS (pH 7.4). Brains were rapidly removed and immersion fixed for 24 h in freshly prepared 4% paraformaldehyde. The brains were then incubated for 24 h in 30% sucrose to cyroprotect them. For tyrosine hydroxylase immunohistochemistry, tissue blocks were cut and mounted in a Leitz cryostat and sectioned using the Paxinos mouse brain atlas as a guide (Paxinos and Franklin, 2001). Tissue sections to be used for tyrosine hydroxylase immunochemistry were selected from the striatal block (Bregma +0.14 at level of anterior commissure to Bregma +1.18); and hippocampal and midbrain block (Bregma −2.8 to −3.46) and the cerebellar/pons block (Bregma −5.84 to −6.24). For TUNEL staining, sagittal sections of 25-μm thickness were placed on Superfrost/Plus Microscope Slides (precleaned) and processed with immunohistochemical staining methods as described below.

2.11. Immunohistochemistry

Mouse brains were placed in ice-cold aluminum brain molds and cut into 2 mm coronal blocks. These tissue blocks were mounted in a cryostat and sectioned using a mouse brain atlas as a guide (Paxinos and Franklin, 2001). In several mouse brains,

tissue was blocked into two mid-sagittal parts and tissue sections (25 μm thin) were cut in the parasagittal plane to include the entire extent of striatum, pallidum and midbrain. Tissue sections to be used for tyrosine hydroxylase immunochemistry were selected from the striatal block (Bregma +0.14 at level of anterior commissure to Bregma +1.18); and hippocampal and midbrain block (Bregma −2.8 to −3.46) and the cerebellar/pons block (Bregma −5.84 to −6.24). For TUNEL staining sections were sampled from all the blocks encompassing forebrain to cerebellum and brainstem. Thin sections (25 μm) were placed on Superfrost/Plus Microscope Slides (precleaned) and processed by using the staining method described below.

2.11.1. Tyrosine hydroxylase (TH) immunoreactivity

Tissue sections were fixed for 30 min at room temperature in 4% paraformaldehyde prepared on PBS (pH 7.4) and then transferred to PBS containing 5% sucrose. After 15 min of incubation sections were treated with 10% H_2O_2 in 95% MeOH for 30 min at room temperature to destroy endogenous peroxidase. Then sections were blocked at room temperature during 60 min with 10% goat serum (Sigma Chemicals, MI) prepared on PBS containing 0.3% Triton X-100. Rabbit anti-tyrosine hydroxylase (Pel-Freez Biologicals, Arkansas) was the primary antibody (1:1000) and it was prepared in PBS containing 10% goat serum and 0.3% Triton X-100. The sections were incubated with primary antibody overnight at 4 °C and then washed in three changes of PBS for 10 min each. Goat anti-rabbit (Chemicon, CA) secondary antibody was prepared on PBS/Triton X-100 buffer (1:300) and incubated with samples for 60 min at room temperature. Then sections were washed for 10 min in three changes of PBS, treated with avidin–biotin-complex (Vectastain ABC Kit (Peroxidase Standard*), Vector Labs, CA) for 60 min and developed with 3,3′-diaminobenzidine (DAB Substrate Kit, Vector Labs, CA) at room temperature during 2–5 min. Finally the sections were rinsed with distilled water to stop reaction and then dehydrated in ethanol, and cleared in xylene. Controls for nonspecific staining were performed for evaluation in which either primary or secondary antibody was applied alone.

2.11.2. TUNEL assay

TUNEL staining was performed following the methods described in ApopTag Plus Fluorescein In Situ Apoptosis Detection Kit (S7111) and ApopTag Peroxidase In Situ Apoptosis Detection Kit (S7100) (Chemicon, CA). Slide-mounted tissue sections were post-fixed in precooled ethanol:acetic acid (2:1) for 5 min at −20 °C in a Coplin jar and rinsed two times for 5 min with PBS. For ApopTag Peroxidase staining slices were quenched in 3.0% hydrogen peroxidase in PBS for 5 min at room temperature and rinsed twice with PBS for 5 min each time. Equilibration buffer was immediately applied directly to the specimen for 20 s at room temperature. TdT enzyme was pipetted onto the sections following by incubation in a humidified chamber for 1 h at 37 °C. Specimens were placed in a Coplin jar containing working strength stop/wash buffer and incubated for 10 min at room temperature. After triple rinsing in PBS, the sections were incubated with anti-digoxigenin conjugate (fluorescence) or anti-digoxigenin peroxidase conjugate accordingly in a humidified chamber for 30 min at room temperature. The specimen for fluorescence apoptosis staining were rinsed with PBS (4× 2 min) and mounted on a glass cover slip with Vectashield mounting medium containing DAPI or PI (Vector Labs, CA). The specimens for peroxidase staining were rinsed with PBS (4× 2 min) and color was provided in peroxidase substrate (DAB Substrate KIT for peroxidase, Vector Labs). Then sections were rinsed in three changes of dH_2O for 1 min each wash and counterstained in methyl green (Vector Labs). The specimens were dehydrated and mounted under a glass coverslip in mounting medium. Samples were then examined with bright field microscopy or in the case of fluorescently tagged antibodies, with a Zeiss Scanning Confocal microscope (Model LSM510).

2.11.3. Rabbit anti-DARPP32

Sections were immunostained for DARPP32, a protein expressed by striatal neurons and which has been used to characterize effects of toxicants on striatal neurons (Haug et al., 1998; Stefanova et al., 2003). Cryosections were rinsed in PBS three times for 10 min each wash. Then the sections were incubated with ''blocking'' solution (PBS containing 10% goat serum (Sigma, Missouri), 0.3% Triton X-100) at room temperature for 60 min. Primary antibody *rabbit anti-DARPP32* (Chemicon, CA) diluted in carrier solution (PBS, goat serum, Triton X-100, primary antibody 1:300) was placed onto the sections and incubated overnight at 4 °C.

Secondary antibody *goat anti-rabbit secondary* (Alexa Fluor 594 (rodamine) Chemicon, CA) was applied to the slides (PBS, Triton X-100, secondary antibody—1:300) for 60 min at room temperature. Finally, the sections were rinsed with PBS (3× 10 min) and mounted on a glass cover slip with Vectashield mounting medium containing DAPI (Vector Labs, CA). Appropriate controls without primary antibodies were also prepared to assess nonspecific immunohistochemical staining. In some sections, propidium iodide (PI) from Molecular Probes (Eugene, OR) was used to counterstain nucleic acid. Laser Scanning confocal microscopy (Zeiss LSM 510) was used to resolve TUNEL-stained tissues counterstained with PI.

2.12. Statistical analysis

The results were reported as mean ± S.E.M. for at least five individual samples of specific brain regions, assayed in duplicate. Two-way ANOVA was performed to assess the contribution of brain region, time of analysis and their interaction on variance. Post-hoc *t*-tests with Bonferroni corrections were performed to compare values at each time point to control (untreated) values.

For electrophoresis, two different gels were run. The differences between samples were analyzed by the Student's *t*-test, and a $p < 0.05$ was considered as statistically significant. The Pearson correlation coefficients between DNA repair

Table 1
Development of TBARS response in different regions of mouse brain following i.p. administration of 3.5 mg/kg of OTA

Brain regions	TBARS (pmol/mg protein)			
	Control	6 h	24 h	72 h
CB	2.44 ± 0.2	3.99 ± 0.35*	5.54 ± 0.48*	8.54 ± 0.77*
PM	2.41 ± 0.17	4.80 ± 0.43*	6.09 ± 0.55*	9.13 ± 0.89*
HP	2.23 ± 0.21	4.69 ± 0.4*	6.03 ± 0.52*	8.57 ± 0.88*
MB	3.17 ± 0.28	4.22 ± 0.33*	6.09 ± 0.53*	9.16 ± 0.81*
CP	2.65 ± 0.22	3.58 ± 0.32*	5.63 ± 0.49*	8.39 ± 0.79*
CX	3.19 ± 0.27	4.01 ± 0.41*	6.78 ± 0.63*	10.31 ± 0.98*

* The values are significantly ($p < 0.05$) different compared to controls. All results represented by mean ± S.E.M.

(OGG1) and basal DNA damage (comet assay) across brain regions were determined at each time point by correlation analysis using GraphPad Software, Inc. (Sorrento, CA).

3. Results

Administration of OTA at doses less than 6 mg/kg i.p. (below the reported LD50 of 39.5 mg/kg i.p. in mice, Moroi et al., 1985) did not elicit obvious alterations in mouse behavior and locomotor activity at any time up to 3 days after treatment. Behavior was not measured instrumentally, but was based on visual inspections over the course of 3 days and response to handling. In particular, there was no abnormal posturing or clasping of limbs when mice were picked up by the tail.

Administration of a single dose of OTA (3.5 mg/kg i.p.) rapidly evoked oxidative stress across all brain regions. TBARS levels, indicators of lipid peroxidation, increased in a monophasic time-dependent manner in all brain regions of animals exposed to OTA as compared to control mice (Table 1). This same dose of OTA caused a rapid upregulation of SOD activities in all regions of brain, with peak values reached after 24 h. However, the elevation of the SOD antioxidative response was maintained only for a short time, returning to control levels or below after 72 h (Table 2).

Oxidative DNA damage, estimated from the comet assay (Fig. 2), was increased early across all brain regions (Fig. 3) and remained elevated at all time points. Peak elevation was

Table 2
Development of SOD response in different regions of mouse brain during intoxication caused by i.p. administration of 3.5 mg/kg of OTA

Brain regions	SOD (U/g protein)			
	Control	6 h	24 h	72 h
CB	0.39 ± 0.04	0.38 ± 0.03	0.71 ± 0.07*	0.35 ± 0.03
PM	0.557 ± 0.05	0.61 ± 0.05	0.8 ± 0.08*	0.37 ± 0.03
HP	0.37 ± 0.03	0.39 ± 0.03	0.81 ± 0.07*	0.33 ± 0.03
MB	0.36 ± 0.03	0.44 ± 0.04	0.79 ± 0.07*	0.34 ± 0.02
CP	0.34 ± 0.02	0.36 ± 0.03	0.73 ± 0.06*	0.32 ± 0.02
CX	0.53 ± 0.04	0.55 ± 0.04	0.91 ± 0.08*	0.36 ± 0.04

* The values are significantly ($p < 0.05$) different compared to controls. All results represented by mean ± S.E.M.

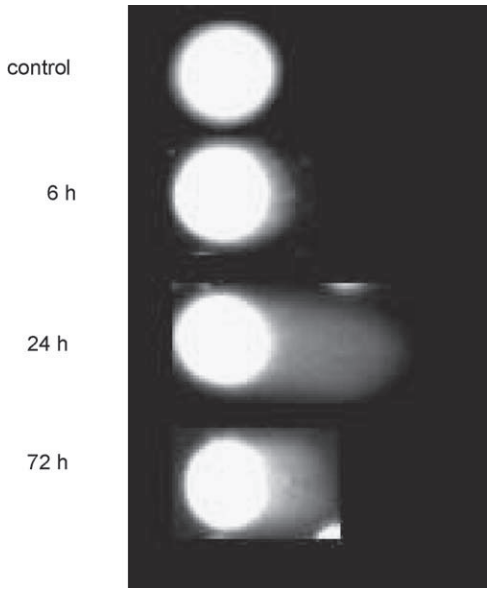

Fig. 2. Representative photomicrographs of "comets" in the substantia nigra obtained at 6, 24 and 72 h after OTA injection (3.5 mg/kg, i.p.).

observed at 24 h where the magnitude of increase ranged from 1.8 to 2.9 times the control levels. The MB, CP and HP showed the highest levels of oxidative DNA damage.

Concomitant with the increased levels of oxidative DNA damage, the DNA repair enzyme OGG1 was significantly decreased across all brain regions at 6 h with a gradual return to near normal levels by 72 h (Fig. 4). The activity of OGG1 across the six brain regions was inversely correlated to basal levels of DNA damage at all time points except for 72 h (the Pearson correlation coefficients were −0.88 at 0 h; −0.89 at 6 h; −0.85 at 24 h; −0.45 at 72 h—see Fig. 5). Oxidative DNA repair activity recovered completely by 72 h in CB but

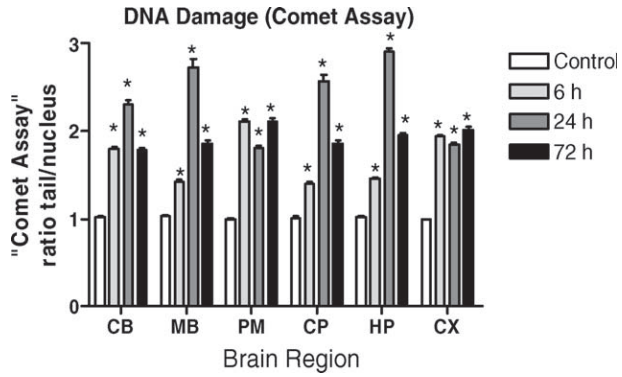

Fig. 3. Time course of effects of OTA on DNA damage across six brain regions mice following administration of OTA (3.5 mg/kg, i.p.). The extent of DNA damage was calculated from relative changes in length of comet tails. The mean ± S.E.M. was determined from the average of 50 cells calculated for three animals in each experimental group (control, 6, 24 and 72 h). Two-way ANOVA revealed that brain region and time each contributed significantly to the variance ($p < 0.0001$); there was no statistically significant interaction between time course and region. Post-hoc comparison of values at each time point compared to controls revealed significant increases at each time point for each region (asterisks indicate $p < 0.05$; t-test with Bonferroni correction for multiple comparisons).

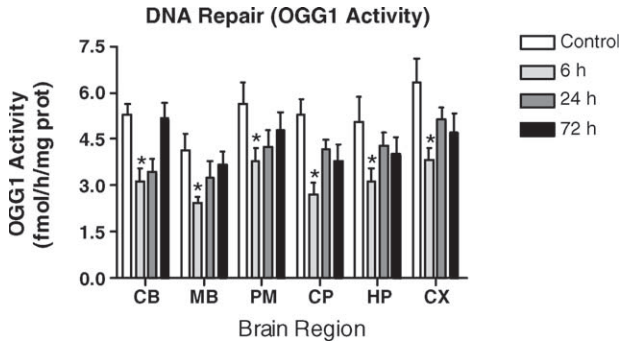

Fig. 4. Time course of OTA effects on OGG1 activity across specific brain regions. Results are expressed as mean ± S.E.M. ($n = 4$–6 samples per brain region). Two-way ANOVA revealed that brain region and time each contributed significantly to the variance ($p < 0.0001$); there was no statistically significant interaction between time course and region. Post-hoc comparison of values at each time point compared to controls revealed significant decreases at 6 h in each region (asterisks indicate $p < 0.05$; *t*-test with Bonferroni correction for multiple comparisons).

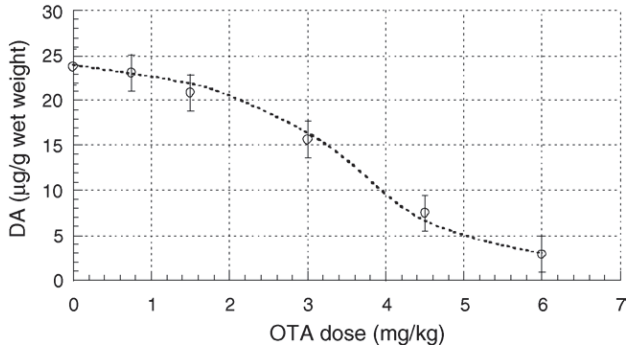

Fig. 6. Dose–response curve obtained following i.p. administration of OTA. DA concentration was measured in CP of ICR mice 24 h after administration of OTA. The results are expressed as mean ± S.E.M. Data averaged for five animals.

remained depressed in all other regions despite a trend towards recovery. The CP, CX and HP exhibited the least degree of recovery of OGG1 activity; at 72 h, the CP remained inhibited by 28%, the CX by 26% and the HP by 21% compared to control OGG1 levels.

In light of the long-standing premise that the nigro-striatal DA system is vulnerable to oxidative stress (a view that has been recently challenged, Ahlskog, 2005), we measured levels of DA and its metabolites in the striatum. OTA administration resulted in a dose-dependent decrease in striatal (caudate/putamen) DA with an ED50 of 3.2 mg/kg (Fig. 6). A time-course study of the effects of a single dose (3.5 mg/kg i.p.) revealed an early (6 h) 1.38-fold elevation of

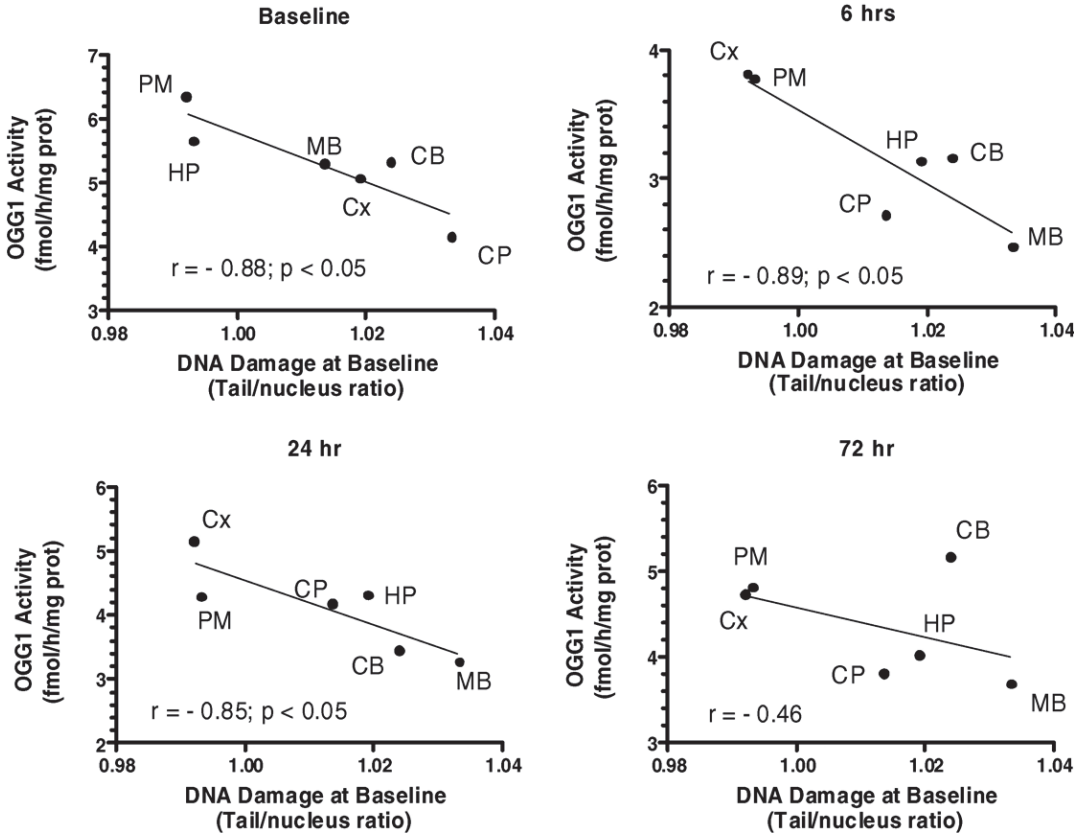

Fig. 5. Relationship between DNA repair (OGG1) and basal levels of oxidative damage in six brain regions. Each panel plots OGG1 activity against the baseline oxidative DNA damage (tail/nucleus ratio of the comet assay) in each brain region at 6, 24 and 72 h after a single dose of OTA (3.5 mg/kg). Pearson correlation coefficients were determined for each time point shown in the four panels. There was a significant inverse correlation between DNA repair activity and baseline level of DNA damage across regions at all time points except 72 h.

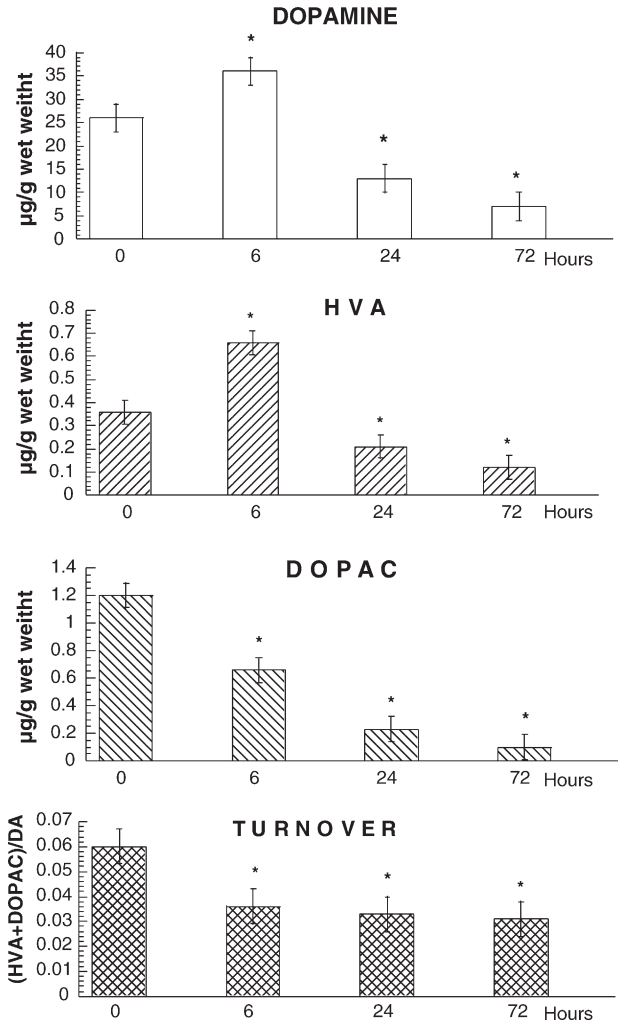

Fig. 7. Effect of OTA administration (3.5 mg/kg, i.p.) on DA metabolism during time course of developed intoxication in brain of ICR mice. Asterisks indicate significance of differences against control ($p < 0.05$). The results are expressed as mean ± S.E.M. ($n = 6$).

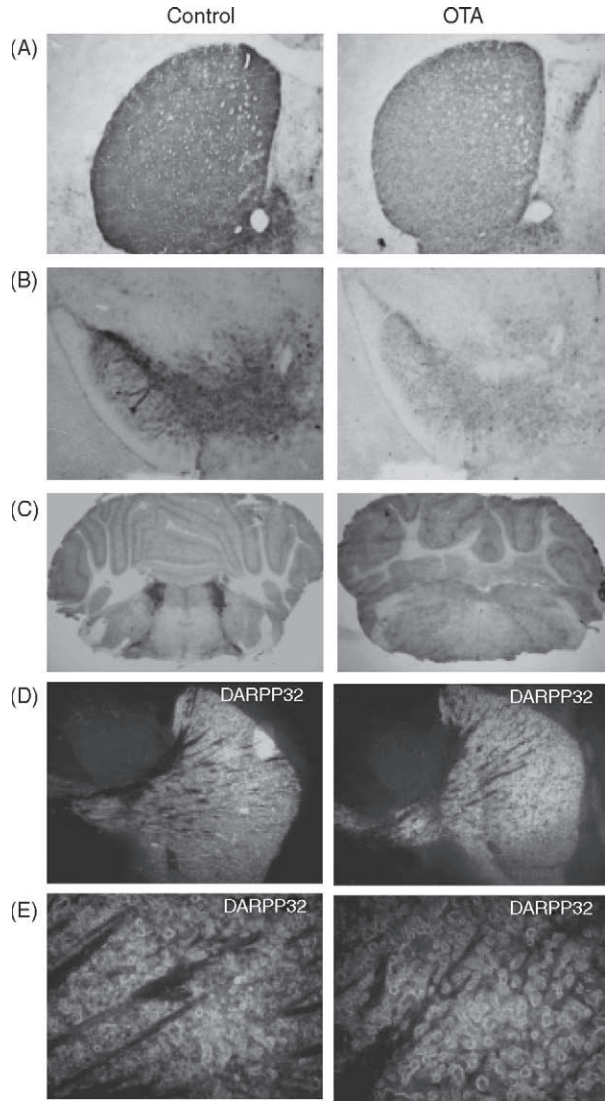

Fig. 8. Representative photomicrographs of TH immunoreactivity in the caudate putamen (row A), substantia nigra (row B) and locus ceruleus (row C) obtained 72 h after OTA injection (3.5 mg/kg, i.p.). Controls are in the left-hand panels. Intensity of TH immunoreactivity is decreased in all three loci in mice treated with OTA. DARPP32 immunohistochemistry is shown in rows D and E. Parasagittal cut through striatum (CP) showing no difference in DARPP32 signal intensity and distribution in OTA-treated compared to control mouse brains (magnification in row D = 40×; in row E = 200×).

DA as compared to control (Fig. 7). After 24 h, DA concentration dropped to 46% of control levels and declined even further by 72 h. A similar kinetic profile was recorded for HVA, while DOPAC levels did not increase at 6 h but showed a steady decline. The turnover of DA calculated as ratio of (HVA + DOPAC)/DA was significantly reduced at all time points (Fig. 7).

Catecholaminergic cells and terminals in the SN, CP and locus ceruleus were affected by OTA as evidenced by a qualitative decrease in tyrosine hydroxylase (TH) immunoreactivity in those structures (Fig. 8, rows A–C). However, the decreased immunostaining was not a result of OTA-induced cell death because TUNEL staining across these and other brain regions failed to reveal apoptotic nuclei (data not shown). DARPP32 immunostaining of cells of the striatum and midbrain (SNpars reticulata) did not reveal differences between OTA and control brains, indicating that there was no direct cytopathic effect on this population of neurons by 72 h after administration (Fig. 8, rows D and E).

4. Discussion

Administration of OTA, at a single dose (3.5 mg/kg) that is approximately 10% of the reported LD50, resulted in widespread oxidative stress across six brain regions. This was evidenced by significant increases in lipid peroxidation and oxidative DNA damage across all brain regions. Furthermore, OTA treatment elicited an early and sustained surge in activity of SOD, a major oxyradical scavenger, across all brain regions. Unlike the monophasic SOD activation, the oxidative DNA repair response exhibited a biphasic response, with an initial inhibition of OGG1 activity followed by a trend towards recovery to normal levels after 3 days. This is quite different

than the acute effects of another pro-oxidant agent, diethyl maleate (DEM), which elicited an early (6 h after injection) and significant upregulation of OGG1 in mouse CB, CX, PM, but not in MB, CP or HP, despite equally decreased glutathione levels in all brain regions (Cardozo-Pelaez et al., 2002). In addition, the DNA repair response to rubratoxin-A (RTA), a mycotoxin with poorly understood complex mechanisms of action in brain, was similar but not identical to that of diethyl maleate. Administration of a single dose of RTA resulted in significant upregulation of the DNA repair enzyme OGG1 in CB, CP, and CX, but not in HP, MB and PM at 24 h, in the presence of *decreased or unchanged levels* of lipid peroxidation in all regions (Sava et al., 2004). In the present study, the OGG1 activity was suppressed equally in all brain regions and only the CB recovered to baseline levels by 72 h, while other regions (CP, HP and CX) approached baseline but stayed mildly suppressed. It should be pointed out that the results in the DEM and RTA experiments cannot be directly compared with the present findings because only a single time point was assessed (6 h in the DEM study and 24 h in the RTA study) and no measurements of DA levels in striatum were made in those earlier experiments (Sava et al., 2004).

Based on our previous work with diethyl maleate and rubratoxin-A, we had expected that the DNA repair response to OTA would show that some regions of brain were more capable of OGG1 upregulation than others. Our working hypothesis was based on the concept that variation in DNA repair was a potential factor in determining neuronal vulnerability; deficient DNA repair processes have been associated with Parkinson's disease (PD) as well as with other neurodegenerative diseases such as Alzheimer's disease, amyotrophic lateral sclerosis (ALS) and Huntington's disease (HD) (Lovell et al., 2000; Mazzarello et al., 1992; Robbins et al., 1985). In addition, we have previously shown that the uneven distribution of oxidative DNA damage across brain regions caused by endogenous or exogenous factors was determined, in part, by the intrinsic capacity to repair oxidative DNA damage (Cardozo-Pelaez et al., 1999, 2000). In those earlier studies, and in the present report, we focused on oxyguanosine glycosylase (OGG1), a key enzyme involved in the repair of the oxidized base, 8-hydroxy-2′deoxoguanosine (oxo8dG). This reaction results in hydrolysis of the *N*-glycosylic bond between the 8-oxoG and deoxyribose, releasing the free base and leaving an apurinic/apyrimidinic (AP) site in DNA. Such AP sites are cytotoxic and mutagenic, and must be further processed. Some DNA glycosylases also have an associated AP lyase activity that cleaves the phosphodiester bond 3′ to the AP site (Dianov et al., 1998). Un-repaired DNA damage in post-mitotic cells, such as neurons, can result in disruption of transcriptionally active genes, cellular dysfunction and apoptosis (Hanawalt, 1994). Hence it was reasonable to hypothesize that diminished DNA repair capacity in populations of neurons would be associated with increased vulnerability to potentially genotoxic agents. Since the CP and MB showed a relatively diminished OGG1 activity and increased oxidative DNA damage (comet assay), we postulated that the DA terminals of the striatum would suffer damage.

This concept was supported by the report of increased oxidative DNA damage in substantia nigra and striatum in post-mortem brain from PD cases (Sanchez-Ramos et al., 1994), and by the observation that MB and CP were less able to upregulate OGG1 repair activity in response to the pro-oxidant, diethylmaleate (Cardozo-Pelaez et al., 2002). To further test this hypothesis, we measured the effects of OTA on striatal DA levels. Administration of OTA caused a dose-dependent decrease of striatal DA and a decrease in DA turnover. The nearly 50% reduction in striatal DA caused by a single dose (3.5 mg/kg i.p.) did not produce observable changes in daytime mouse behavior or locomotor activity, though it is likely that more sensitive, quantitative measures of behavior may reveal alterations. This dose of OTA also resulted in diminished TH immunoreactivity in the CP and MB as well as in the locus ceruleus (which contains noradrenergic neurons). The effects of OTA on catecholaminergic systems appeared to reflect a potentially reversible action rather than a cytotoxic effect because we found no evidence of cell death by 72 h. There were no apoptotic profiles found in SN and CP or any other region of the brain. In addition, there did not appear to be cytotoxic effects on striatal neurons identified by DARPP32 immunostaining.

It may be that the more rapid return of OGG1 activity to normal by 3 days in CB reflects an uneven distribution of the mycotoxin across brain regions. In the present report, the distribution of the toxin itself across brain regions was not investigated. However, previously published reports indicate that the cerebellum, ventral midbrain, and striatum accumulate the highest levels of OTA after 8 days of intragastric administration of a low dose (289 μg/kg/day) (Belmadani et al., 1998). Cerebellar concentrations of OTA accounted for 34% of the total brain OTA and one might expect that this structure would exhibit the greatest degree of oxidative stress and decreased capacity to repair oxidative DNA damage. On the contrary, the present findings demonstrate that the cerebellum exhibited complete recovery of OGG1 activity whereas other regions, reported to accumulate much lower levels of OTA, did not recover DNA repair capacity to as great an extent. Similarly, it has been reported that the cerebellum exhibited the least degree of cytotoxicity evidenced by LDH release; the greatest release of LDH was reported to be in ventral midbrain, hippocampus, and striatum which accumulated much less OTA than the cerebellum (Belmadani et al., 1998). Hence the relationship between regional concentration of OTA and regional vulnerability to the toxin is not clear.

A potential explanation for the observations reported here relates to bioenergetic compromise evoked by OTA. This mycotoxin has been reported to inhibit succinate-dependent electron transfer activities of the respiratory chain, but at higher concentrations will also inhibit electron transport at Complex I (Aleo et al., 1991; Wei et al., 1985). The nigro-striatal dopaminergic system is well known to be especially vulnerable to the mitochondrial toxicants, MPTP and rotenone, especially when the latter toxicant is administered chronically at low doses (Betarbet et al., 2000; Hasegawa et al., 1990; Vyas et al., 1986). Other mitochondrial poisons like nitroproprionic acid

and malonate interfere with succinate dehydrogenase/Complex II. These Complex II inhibitors result in lesions primarily localized to striatum (Calabresi et al., 2001; Schulz et al., 1996). Bioenergetic compromise may lead to persistent activation of NMDA receptors which results in excitotoxicity mediated by the neurotransmitter glutamate in regions of brain richly innervated by glutamatergic fibers, accounting for the vulnerability of the striatum and pallidum, and possibly the SN (Greenamyre et al., 1999; Turski and Turski, 1993). In addition, Ca^{2+} entering neurons through NMDA receptors has 'privileged' access to mitochondria, where it causes free-radical production and mitochondrial depolarization (Greenamyre et al., 1999). Hence the bioenergetic compromise induced by OTA may be responsible for the generation of free radicals and reactive oxygen species that resulted in global oxidative damage to DNA and lipids, as reported here and damage to proteins through generation of oxygen free radicals and nitric oxide, as reported elsewhere (Bryan et al., 2004; Thomas and Mallis, 2001).

Of course OTA may also be toxic through other mechanisms. Due to its chemical structure (chlorodihydroisocoumarin linked through an amide bond to phenylalanine), OTA inhibits protein synthesis by competition with phenylalanine in the aminoacylation reaction of phenylalanine-tRNA (Bunge et al., 1978; Creppy et al., 1983a) and phenylalanine hydroxylase activity (Creppy et al., 1990). These actions could lead to impairment of the synthesis of DOPA, dopamine and catecholamines or enzymes involved in metabolism of DA. Interestingly, the initial effect of OTA was to release DA resulting in increased striatal DA and HVA levels at 6 h, but with a decreased level of striatal DOPAC. It is known that DOPAC levels in striatum decline when DA nerve terminals are exposed to drugs which release newly synthesized DA, possibly because intraneuronal monoamine oxidase is deprived of its main substrate (Zetterstrom et al., 1988). Longer term studies will be required to determine the extent to which the effects of OTA on striatal DA and its metabolites is permanent or reversible.

To summarize, OTA administered at a dose that is 10% of the LD50, resulted in significant reduction of striatal DA, DA turnover and TH immunoreactivity in catecholaminergic neurons and fibers. This was not associated with apoptosis in SN, CP, HP, CB or with loss of striatal neuron immunostaining for DARPP32. OTA evoked pronounced global oxidative stress, possibly related to its inhibition of mitochondrial function. Regional variation in DNA repair did not appear to explain effects on catecholaminergic neurons. The vulnerability of the nigro-striatal system to OTA remains unclear and many questions remain to drive on-going and future investigations. For example, what are the long-term consequences of chronic administration of more clinically relevant low doses of OTA? Does a rigid-akinetic syndrome develop and is it reversible? Given that data derived from analysis of six macro-dissected brain regions are crude approximations for the cellular and molecular events occurring in specific populations of neurons, it will be important to develop refined sampling methods, including microdissection of specific neuro-anatomical loci and laser capture microdissection techniques for analysis of specific neuronal phenotypes.

Acknowledgements

This study was supported by USAMRMC #03281031 and a VA Merit Review Grant.

References

Ahlskog JE. Challenging conventional wisdom: the etiologic role of dopamine oxidative stress in Parkinson's disease. Mov Disord 2005;20:271–82.

Aleo MD, Wyatt RD, Schnellmann RG. Mitochondrial dysfunction is an early event in ochratoxin A but not oosporein toxicity to rat renal proximal tubules. Toxicol Appl Pharmacol 1991;107:73–80.

Arora RG, Frolen H, Fellner-Feldegg H. Inhibition of ochratoxin A teratogenesis by zearalenone and diethylstilboestrol. Food Chem Toxicol 1983;21:779–83.

Belmadani A, Tramu G, Betbeder AM, Steyn PS, Creppy EE. Regional selectivity to ochratoxin A, distribution and cytotoxicity in rat brain. Arch Toxicol 1998;72:656–62.

Betarbet R, Sherer TB, MacKenzie G, Garcia-Osuna M, Panov AV, Greenamyre T. Chronic systemic pesticide exposure reproduces features of Parkinson's disease. Nat Neurosci 2000;3:1301–6.

Bryan NS, Rassaf T, Maloney RE, Rodriguez CM, Saijo F, Rodriguez JR, et al. Cellular targets and mechanisms of nitros(yl)ation: an insight into their nature and kinetics in vivo. Proc Natl Acad Sci USA 2004;101:4308–13.

Bunge I, Dirheimer G, Roschenthaler R. In vivo and in vitro inhibition of protein synthesis in *Bacillus stearothermophilus* by ochratoxin A. Biochem Biophys Res Commun 1978;83:398–405.

Calabresi P, Gubellini P, Picconi B, Centonze D, Pisani A, Bonsi P, et al. Inhibition of mitochondrial complex II induces a long-term potentiation of NMDA-mediated synaptic excitation in the striatum requiring endogenous dopamine. J Neurosci 2001;21:5110–20.

Cardozo-Pelaez F, Brooks PJ, Stedeford T, Song S, Sanchez-Ramos J. DNA damage, repair, and antioxidant systems in brain regions: a correlative study. Free Radic Biol Med 2000;28:779–85.

Cardozo-Pelaez F, Song S, Parthasarathy A, Hazzi C, Naidu K, Sanchez-Ramos J. Oxidative DNA damage in the aging mouse brain. Movement Disord 1999;14:972–80.

Cardozo-Pelaez F, Stedeford TJ, Brooks PJ, Song S, Sanchez-Ramos JR. Effects of diethylmaleate on DNA damage and repair in the mouse brain. Free Radic Biol Med 2002;33:292–8.

Cascio C, Guarneri R, Russo D, De Leo G, Guarneri M, Piccoli F, et al. Pregnenolone sulfate, a naturally occurring excitotoxin involved in delayed retinal cell death. J Neurochem 2000;74:2380–91.

Creppy EE, Chakor K, Fisher MJ, Dirheimer G. The myocotoxin ochratoxin A is a substrate for phenylalanine hydroxylase in isolated rat hepatocytes and in vivo. Arch Toxicol 1990;64:279–84.

Creppy EE, Kane A, Dirheimer G, Lafarge-Frayssinet C, Mousset S, Frayssinet C. Genotoxicity of ochratoxin A in mice: DNA single-strand break evaluation in spleen, liver and kidney. Toxicol Lett 1985;28:29–35.

Creppy EE, Kern D, Steyn PS, Vleggaar R, Roschenthaler R, Dirheimer G. Comparative study of the effect of ochratoxin A analogues on yeast aminoacyl-tRNA synthetases and on the growth and protein synthesis of hepatoma cells. Toxicol Lett 1983a;19:217–24.

Creppy EE, Stormer FC, Roschenthaler R, Dirheimer G. Effects of two metabolites of ochratoxin A, (4R)-4-hydroxyochratoxin A and ochratoxin alpha, on immune response in mice. Infect Immun 1983b;39:1015–8.

Dianov G, Bischoff C, Piotrowski J, Bohr VA. Repair pathways for processing of 8-oxoguanine in DNA by mammalian cell extracts. J Biol Chem 1998;273:33811–6.

Dirheimer G, Creppy EE. Mechanism of action of ochratoxin A. IARC Sci Publ 1991;171–86.

Elstner EF, Heupel A. Inhibition of nitrite formation from hydroxyl-ammonium chloride: a simple assay for superoxide dismutase. Anal Biochem 1976;70:616–20.

Fukui Y, Hayasaka S, Itoh M, Takeuchi Y. Development of neurons and synapses in ochratoxin A-induced microcephalic mice: a quantitative assessment of somatosensory cortex. Neurotoxicol Teratol 1992;14:191–6.

Galtier P. Pharmacokinetics of ochratoxin A in animals. IARC Sci Publ 1991;187–200.

Galtier P, Boneu B, Charpenteau JL, Bodin G, Alvinerie M, More J. Physiopathology of haemorrhagic syndrome related to ochratoxin A intoxication in rats. Food Cosmet Toxicol 1979;17:49–53.

Gautier JC, Holzhaeuser D, Markovic J, Gremaud E, Schilter B, Turesky RJ. Oxidative damage and stress response from ochratoxin a exposure in rats. Free Radic Biol Med 2001;30:1089–98.

Greenamyre JT, MacKenzie G, Peng TI, Stephans SE. Mitochondrial dysfunction in Parkinson's disease. Biochem Soc Symp 1999;66:85–97.

Grosse Y, Baudrimont I, Castegnaro M, Betbeder AM, Creppy EE, Dirheimer G, et al. Formation of ochratoxin A metabolites and DNA-adducts in monkey kidney cells. Chem Biol Interact 1995;95:175–87.

Gupta M, Bandopadhyay S, Paul B, Majumder SK. Hematological changes produced in mice by ochratoxin A. Toxicology 1979;14:95–8.

Hanawalt PC. Transcription-coupled repair and human disease: perspective. Science 1994;266:1957–8.

Hasegawa E, Takeshige K, Oishi T, Murai Y, Minakami S. 1-Methyl-4-phenylpyridinium (MPP+) induces NADH-dependent superoxide formation and enhances NADH-dependent lipid peroxidation in bovine heart submitochondrial particles. Biochem Biophys Res Commun 1990;170: 1049–55.

Haubeck HD, Lorkowski G, Kolsch E, Roschenthaler R. Immunosuppression by ochratoxin A and its prevention by phenylalanine. Appl Environ Microbiol 1981;41:1040–2.

Haug LS, Ostvold AC, Torgner I, Roberg B, Dvorakova L, St'astny F, et al. Intracerebroventricular administration of quinolinic acid induces a selective decrease of inositol(1,4,5)-trisphosphate receptor in rat brain. Neurochem Int 1998;33:109–19.

Hayes AW, Hood RD, Lee HL. Teratogenic effects of ochratoxin A in mice. Teratology 1974;9:93–7.

Hoehler D, Marquardt RR, McIntosh AR, Hatch GM. Induction of free radicals in hepatocytes, mitochondria and microsomes of rats by ochratoxin A and its analogs. Biochim Biophys Acta 1997;1357:225–33.

Kane A, Creppy EE, Roschenthaler R, Dirheimer G. Biological changes in kidney of rats fed subchronically with low doses of ochratoxin A. Dev Toxicol Environ Sci 1986a;14:241–50.

Kane A, Creppy EE, Roschenthaler R, Dirheimer G. Changes in urinary and renal tubular enzymes caused by subchronic administration of ochratoxin A in rats. Toxicology 1986b;42:233–43.

Krogh P. Role of ochratoxin in disease causation. Food Chem Toxicol 1992;30:213–24.

Krogh P, Axelsen NH, Elling F, Gyrd-Hansen N, Hald B, Hyldgaard-Jensen J, et al. Experimental porcine nephropathy. Changes of renal function and structure induced by ochratoxin A-contaminated feed. Acta Pathol Microbiol Scand [A] 1974;1–21.

Kuiper-Goodman T, Scott PM. Risk assessment of the mycotoxin ochratoxin A. Biomed Environ Sci 1989;2:179–248.

Lea T, Steien K, Stormer FC. Mechanism of ochratoxin A-induced immunosuppression. Mycopathologia 1989;107:153–9.

Lebrun S, Follmann W. Detection of ochratoxin A-induced DNA damage in MDCK cells by alkaline single cell gel electrophoresis (comet assay). Arch Toxicol 2002;75:734–41.

Lovell MA, Xie C, Markesbery WR. Decreased base excision repair and increased helicase activity in Alzheimer's disease brain. Brain Res 2000;855:116–23.

Marquardt RR, Frohlich AA. A review of recent advances in understanding ochratoxicosis. J Anim Sci 1992;70:3968–88.

Mazzarello P, Poloni M, Spadari S, Focher F. DNA repair mechanisms in neurological diseases: facts and hypotheses. J Neurol Sci 1992;112:4–14.

Moroi K, Suzuki S, Kuga T, Yamazaki M, Kanisawa M. Reduction of ochratoxin A toxicity in mice treated with phenylalanine and phenobarbital. Toxicol Lett 1985;25:1–5.

Paxinos G, Franklin KBJ. The mouse brain in stereotaxic coordinates. San Diego, CA: Academic Press; 2001.

Petkova-Bocharova T, Chernozemsky IN, Castegnaro M. Ochratoxin A in human blood in relation to Balkan endemic nephropathy and urinary system tumours in Bulgaria. Food Addit Contam 1988;5:299–301.

Pfohl-Leszkowicz A, Chakor K, Creppy EE, Dirheimer G. DNA adduct formation in mice treated with ochratoxin A. IARC Sci Publ 1991;245–53.

Pfohl-Leszkowicz A, Grosse Y, Kane A, Creppy EE, Dirheimer G. Differential DNA adduct formation and disappearance in three mouse tissues after treatment with the mycotoxin ochratoxin A. Mutat Res 1993;289:265–73.

Pitout MJ. The effect of ochratoxin A on glycogen storage in the rat liver. Toxicol Appl Pharmacol 1968;13:299–306.

Robbins JH, Otsuka F, Tarone RE, Polinsky RJ, Brumback RA, Nee LE. Parkinson's disease and Alzheimer's disease: hypersensitivity to X-rays in culture cell lines. J Neurol Neurosurg Psychiatry 1985;48:916–23.

Sanchez-Ramos J, Overvik E, Ames BN. A marker of oxyradical-mediated DNA damage (oxo8dG) is increased in nigro-striatum of Parkinson's disease brain. Neurodegeneration (incorporated into Exp Neurol) 1994;3:197–204.

Sava V, Mosquera D, Song S, Stedeford T, Calero K, Cardozo-Pelaez F, et al. Rubratoxin B elicits antioxidative and DNA repair responses in mouse brain. Gene Expression 2004;11:211–9.

Schindewolf C, Lobenwein K, Trinczek K, Gomolka M, Soewarto D, Fella C, et al. Comet assay as a tool to screen for mouse models with inherited radiation sensitivity. Mamm Genome 2000;11:552–4.

Schulz JB, Henshaw DR, MacGarvey U, Beal MF. Involvement of oxidative stress in 3-nitropropionic acid neurotoxicity. Neurochem Int 1996;29: 167–71.

Smith PK, Krohn RI, Hermanson GT, Mallia AK, Gartner FH, Provenzano MD, et al. Measurement of protein using bicinchoninic acid. Anal Biochem 1985;150:76–85.

Stefanova N, Puschban Z, Fernagut PO, Brouillet E, Tison F, Reindl M, et al. Neuropathological and behavioral changes induced by various treatment paradigms with MPTP and 3-nitropropionic acid in mice: towards a model of striatonigral degeneration (multiple system atrophy). Acta Neuropathol (Berl) 2003;106:157–66.

Stormer FC, Lea T. Effects of ochratoxin A upon early and late events in human T-cell proliferation. Toxicology 1995;95:45–50.

Szczech GM, Hood RD. Brain necrosis in mouse fetuses transplacentally exposed to the mycotoxin ochratoxin A. Toxicol Appl Pharmacol 1981;57:127–37.

Thomas JA, Mallis RJ. Aging and oxidation of reactive protein sulfhydryls. Exp Gerontol 2001;36:1519–26.

Turski L, Turski WA. Towards an understanding of the role of glutamate in neurodegenerative disorders: energy metabolism and neuropathology. Experientia 1993;49:1064–72.

Vyas I, Heikkila RE, Nicklas WJ. Studies on the neurotoxicity of MPTP; inhibition of NAD-linked substrate oxidation by its metabolite, MPP+. J Neurochem 1986;46:1501–7.

Wangikar PB, Dwivedi P, Sharma AK, Sinha N. Effect in rats of simultaneous prenatal exposure to ochratoxin A and aflatoxin B(1). II. Histopathological features of teratological anomalies induced in fetuses. Birth Defects Res B Dev Reprod Toxicol 2004;71:352–8.

Wei YH, Lu CY, Lin TN, Wei RD. Effect of ochratoxin A on rat liver mitochondrial respiration and oxidative phosphorylation. Toxicology 1985;36:119–30.

Zetterstrom T, Sharp T, Collin AK, Ungerstedt U. In vivo measurement of extracellular dopamine and DOPAC in rat striatum after various dopamine-releasing drugs; implications for the origin of extracellular DOPAC. Eur J Pharmacol 1988;148:327–34.